Computer-Based Measurement System for Complex Investigation of Shape Memory Alloy Actuators Behavior

Marek Kciuk and Grzegorz Kłapyta
Silesian University of Technology, Faculty of Electrical Engineering,
Department of Mechatronics,
Poland

1. Introduction

1.1 Basic information

Shape Memory Alloys belong to group of so called "SMART" materials, which became more and more popular last years. The smartness of that kind of materials is defined as possibility of its particular properties stimulation using physical or chemical way. Shape Memory Alloy (SMA) is able to change its size (shape) when temperature is changing. Shape Memory Effect (SME) is macroscopic effect of martensitic transition which overlap inside the material. There are two characteristic states of SMA: low temperature – martensitic – state and high temperature – austenitic – state. Material can be easily plastically deformed by relatively small mechanical force in martensitic state. In opposite, material is strong and very hard to deform in austenitic state - it is only elastic deformation viable. During martensitic transition internal crystal order changes, which causes change of material's properties. Material returning to its natural shape during reverse martensitic transition (from austenitic to martensitic state) can put pressure or perform mechanical work. Complex behavior of SMA materials can be illustrated by thermo-mechanical characteristic (Fig.1).

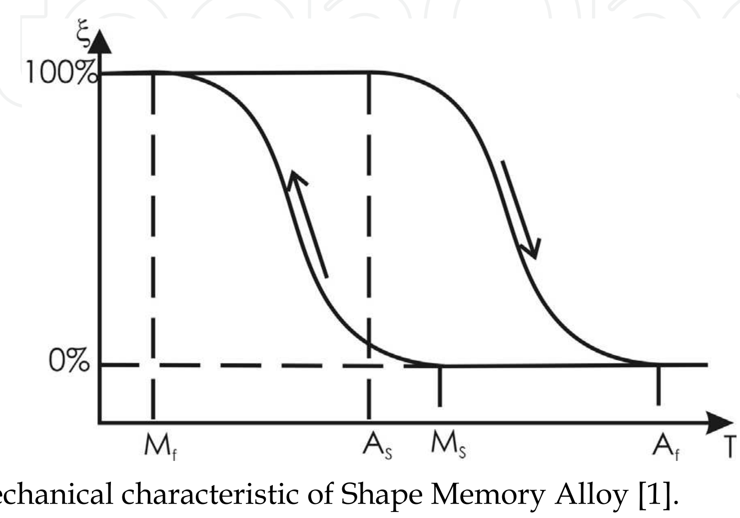

Fig. 1. Thermo-mechanical characteristic of Shape Memory Alloy [1].

Martensitic transition is not isothermal transition. The characteristic is highly nonlinear and exhibit permanent hysteresis loop. There are four important and specific temperature points: M_S and M_f are direct martensitic transition start and finish temperature, while A_S and A_f are reverse martensitic transition start and finish temperature. The highest temperature (A_f) means that all the material is already in austenitic phase; the lowest temperature (M_f) means that all the material is in martensitic phase. ξ is measure of percentage content of molecules in martensitic phase in the volume of the material. For all the temperatures between M_f and A_f the content martensitic fraction (ξ) of material is undefined.

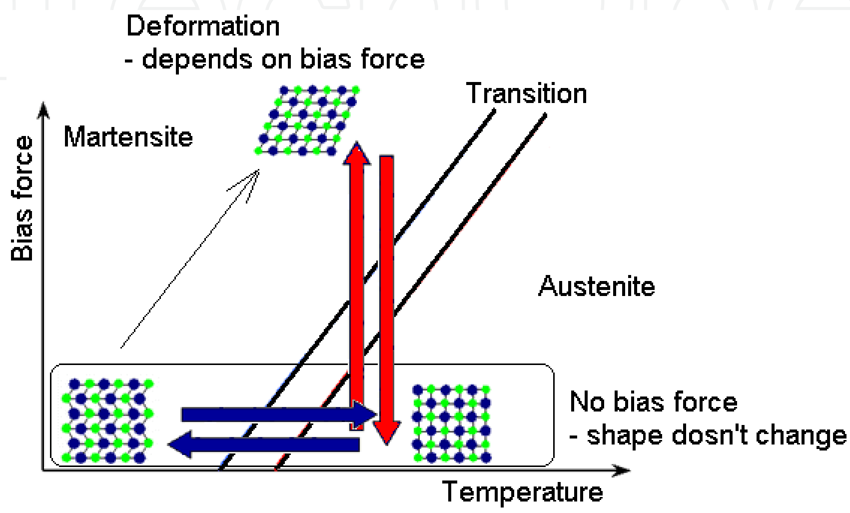

Fig. 2. Shape of SMA material via bias force.

The bias force is important for shape and for martensitic transition parameters. If there is no bias force the macroscopic shape in martensitic state is the same as in austenitic state. If there is a bias force martensitic shape is deformed and is different than austenitic shape. It is presented in Fig. 2.

Important temperatures of martensitic transitions strongly depend on mechanical bias force. The higher bias force is, the higher important temperatures are (there is linear relationship – see Fig.3). Characteristic temperatures under no bias force are marked with "0" subscript.

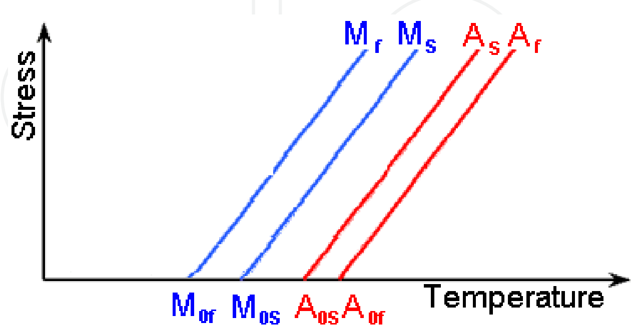

Fig. 3. Characteristic temperatures of martensitic transition via bias force.

Therefore there are two possible ways of transition - one stimulated by temperature, second - stimulated by bias force (respectively blue and red arrows in Fig.2). Temperature stimulated transformation enables to achieve three types of shape: austenitic shape (natural shape, ordered structure of material), martensitic twinned shape (natural shape, unordered structure of material), martensitic deformed shape (deformed shape, unordered structure of material. Bias force stimulated transformation is isothermal and it starts with low bias force and temperature above A0f. Increased mechanical force causes that characteristic temperatures shifts. It is so called superelasticity and enables to achieve only two types of shape: austenitic shape and deformed martensitic shape. This phenomena is presented in Fig.4.

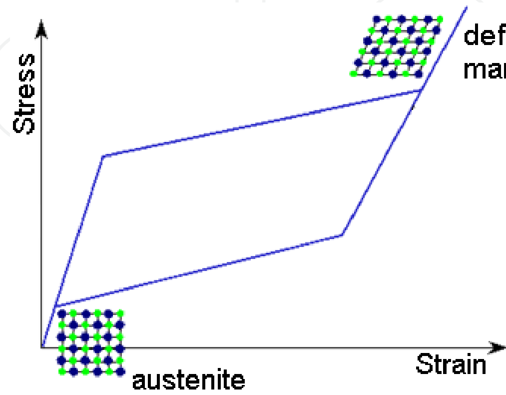

Fig. 4. Superelasticity effect of SMA material.

1.2 Modeling of Shape Memory Alloys

SMAs are already well known and frequently used materials. Different types of mathematical models describe SME behavior. Most popular is modeling based on thermodynamical laws, using different types of free energy equations i.e. Helmholtz's, Gibbs', or Landau'a – Devonshier's [3,6]. There are also mezoscopic models (describing groups of molecules), micromechanical models (describing molecules behavior) and macroscopic models, describing whole material. Ikuta's model describes the state of material by two elements: elastic element and suspension element -the factors are changing with phase changes. There are several types of Ikuta's models (i.e. two layers model, multilayer model, running layers model etc.) [4,5].

Thermodynamical models are the most popular but they are very difficult to implement. They need a lot of parameters and it is hard to use them in control systems.

1.3 Applications

There are two main application groups: SMA works as a sensor or as an actuator. There is also third group of applications, which combine both previously mentioned together.

SMAs are most frequently used as temperature sensors in household, industry devices or air conditioning. Natural hysteresis loop is useful advantage for these kinds of sensors. Threshold temperature mainly depends on material. It is possible to adjust this temperature in some range by mechanical bias force changing.

SMA are also used as active (controlled) or passive (not controlled) actuators. Passive actuators exploit the phenomenon of superelasticity. They are used in civil engineering to protect buildings bridges etc. (e.g. as seismic protection). Passive SMA actuators can suppress vibrations. See Fig.5.

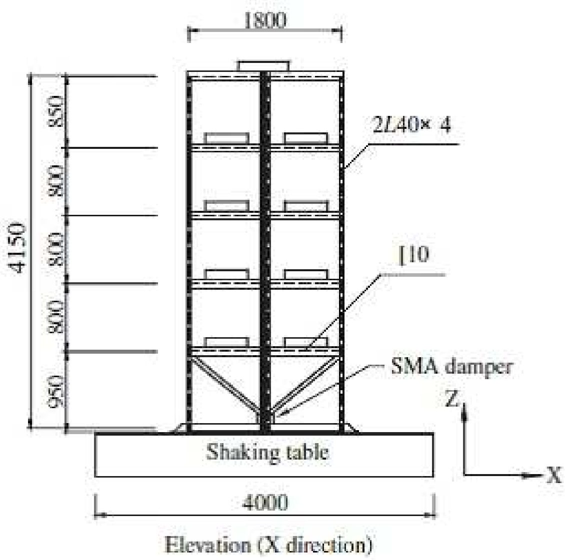

Fig. 5. Comparison of stress distribution of protected and not protected building [15].

Active SMA actuators are popular in mechatronic applications as unconventional drives. They are light-weight actuators with high power to weight ratio. They are able to replace sophisticated electro-mechanical devices in simple tasks. They generate linear displacement in direct way. Sparkles work ensures the safety of work in flammable and wet areas. It is also possible to build light-weight robots (or robotic tools) actuated by SMA. Unconventional robotic hand driven by SMAs is described in [7]. Two types of unconventional mobile robots (snake robot and net robot) are presented in [8, 9]. It is possible to build micro robots made in MEMS technology, actuated by SMAs [10].

2. Measuring stand

Measuring stand for obtaining the complex SMA characteristics was designed and built in Department of Mechatronics at Silesian University of Technology. The stand allows for measurements of static as well as dynamic characteristics of SMA wires. Multiparameter simultaneous measurement enables comparison of different characteristics and allows for assessment of impact of particular parameters on the studied phenomena. Main assumptions for measuring stand project were:

- resistive heating of wire with current constraint,
- possibility of mechanical load changing,
- temperature measurement using infrared camera,
- optical measurement of wire displacement,
- simultaneous measurement of current, voltage, wire displacement and temperature,
- maximum wire length – 900mm,
- minimal mechanical load – 75g,
- maximum wire displacement – 80 mm,
- automatic measurement process with data acquisition system.

Measurement system presented in this paper allows to investigate complex electro-thermo-mechanical characteristics. It is possible to measure electro-mechanical characteristics (length of actuator vs. wire current $L = f(I)$, wire resistance vs. length of actuator $R = f(L)$, etc.), thermo-mechanical characteristic (wire length vs. temperature of actuator $L = f(T)$), electro-thermal characteristic (temperature of actuator vs. supplying current $T = f(I)$), etc. The idea of measurement system is described in Fig.6.

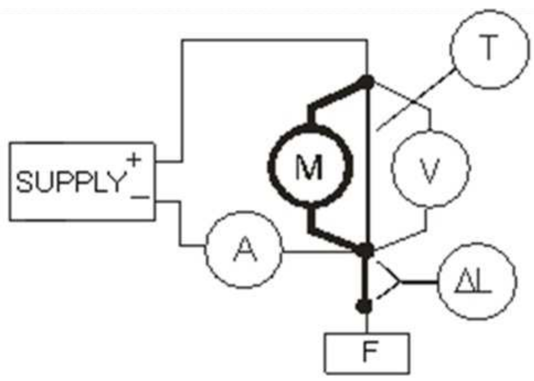

Fig. 6. Idea of measurement system.

There are six main modules: mechanical construction (M) with bias force (F), supply module, and measurement modules: current module (A), voltage module (V), temperature module (T), length changing measurement module (ΔL). Measurement stand is controlled via PC computer in LabVIEW environment. Detailed construction of each module is described below.

Mechanical construction: Design of a stand (Fig.7) allows to place SMA wire (1) between stiff crosspiece (2) and moving piston (3). Gravitational mechanical load can be increased by using additional masses and allows for constant load during measurement process. Base (4), frame (5), and the crosspiece (2) are made of aluminum profiles. Infrared camera (6) is mounted to the base at constant level but it can be shifted horizontally to allow picture sharpness regulation. Electrical circuit is electrically separated from aluminum base by PCV distances. To improve the quality of infrared measurement part of the stand was covered with black cardboard sleeve. In window of Fig.7a. you can see also displacement sensor placed in the bottom part of stand.

Heat supply is done in electrical way, hence SMA wire is a good conductor. According to the Joule-Lenz Law the wire temperature rise is nearly proportional to the square of flowing current. To set the constant temperature in SMA wire the supply system should allow for current stabilization. The power supply PSH-3620A (36V, 20A) was chosen to feed the system. It allows for current as well as for voltage stabilization. Stabilization is switched automatically according to Ohm's law. Measurement stand is closed inside black cartoon shield which guarantees steady air conditions and is helpful for temperature measurements using infrared camera.

Measurement of electrical parameters is done by three precise multimeters Rigol DM3052. It allows for simultaneous measurement of current and voltage of SMA actuator and voltage signal of displacement sensor. Data acquisition and control signals are realized by PC computer. All elements of the measuring system are connected and synchronized by GPIB network (IEEE 488.2 standard). Control program for static measurements was written in G language (LabVIEW environment). For dynamic measurements data recording is performed using digital oscilloscope Tektronix MSO 2024 equipped with four separated channels and digital filter.

(a)

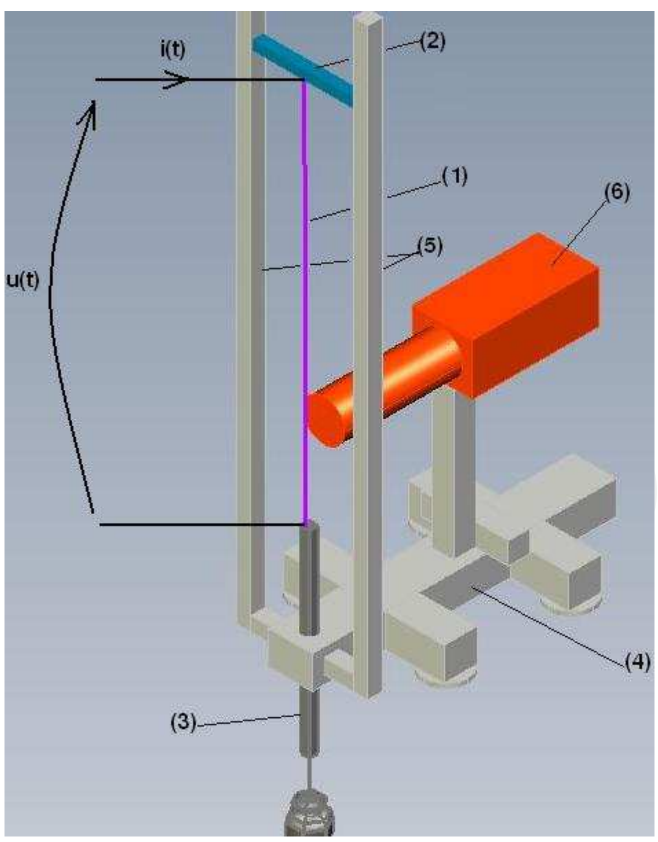

(b)

Fig. 7. Measuring stand: (a)real view; (b)3D model

Temperature measurement is realized using infrared camera Flir A325. It has resolution of 320x240 pixels and can record pictures up to 60Hz. For measuring temperature of very thin wires (50-500μm) special macroscopic lens (closeup 1x) were used. Its surface resolution is 25μm. Camera signal is send to PC computer by Gigabit Ethernet connection (with maximum speed of 1GB/s). IR camera software finds in the image point of the highest temperature and acquires it as the actual temperature of the wire. Additionally, ambient temperature is measured all the time by digital thermometer chip DS18B20, however its result is only displayed but not recorded. Fig.8 presents infrared camera view for SMA wire with 308μm diameter.

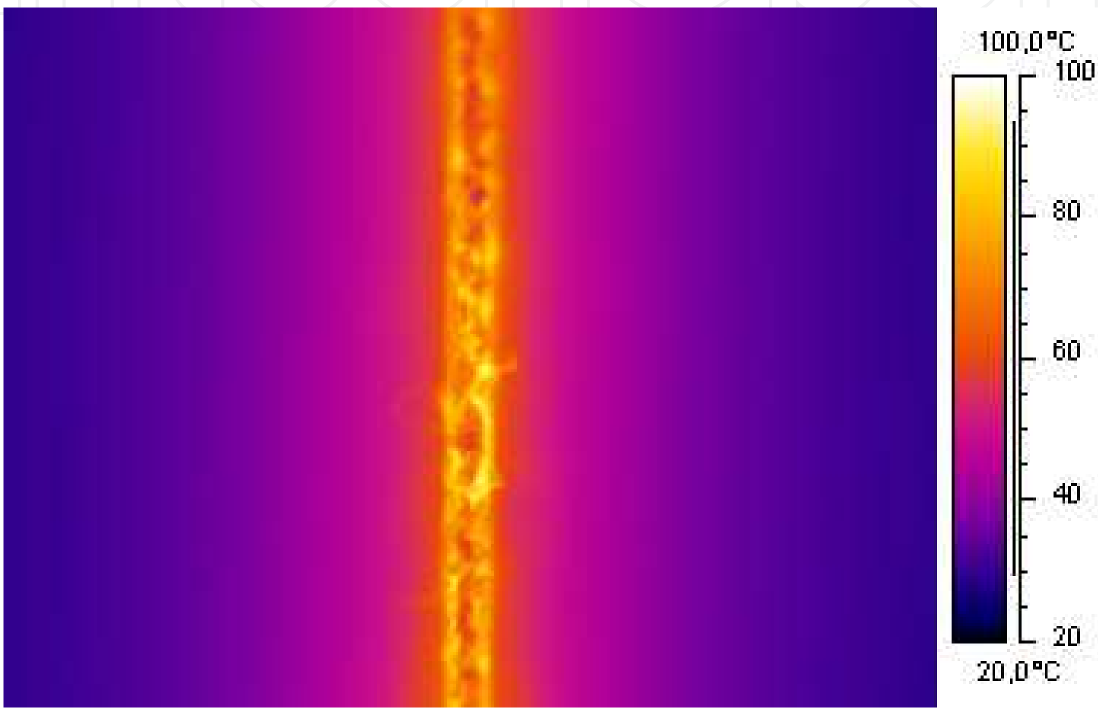

Fig. 8. Infrared camera view for SMA wire with 308μm diameter.

Displacement measurement module is working in two steps. First "displacement-voltage" converter converts displacement into voltage signal, next voltage signal is measured by multimeter. Module consists of optical sensor (converting piston movement into series of pulses), pulses counter, PWM signal generator (PWM signal fulfillment is proportional to number of pulses), lowpass filter and buffer for conditioning signal. Amplitude of converter's external voltage is measured by digital multimeter Rigol DM3052. Movement detection is realized by integrated quadrature optical sensor H9720 and measuring tape with 85 μm resolution scale. Quadrature optical sensor H9720 detects direction of movement based on two geometrically shifted signals (A and B). Pulse counting and PWM generating is realized by 8-bit microcontroller AVR ATmega88. Microcontroller count pulses from one input while second input is used only for direction detection. Pulse counting is realized by detection of (both) signal ramps using external interrupt INT. When ramp is detected both inputs are compared. If their signals have the same value - counter is decreased, if not - it is increased. Block diagram presenting displacement-voltage converter is shown in Fig.9b while idea of pulse counting (with direction detection) is shown in Fig.10.

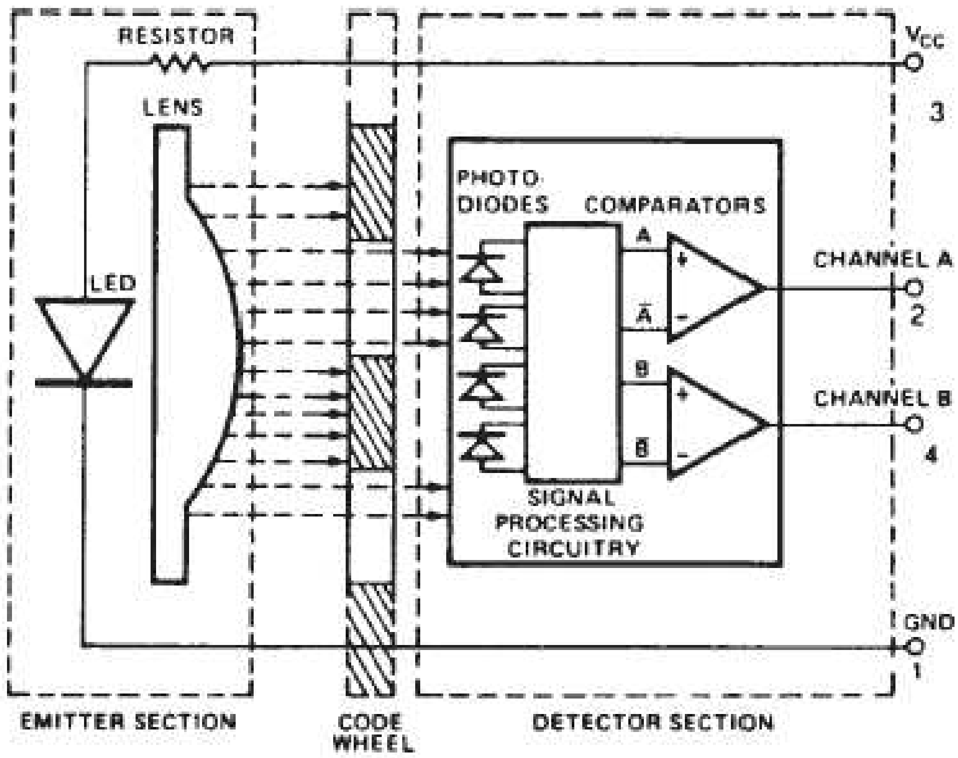

Fig. 9(a). Block diagram of Q9720 sensor. [11]

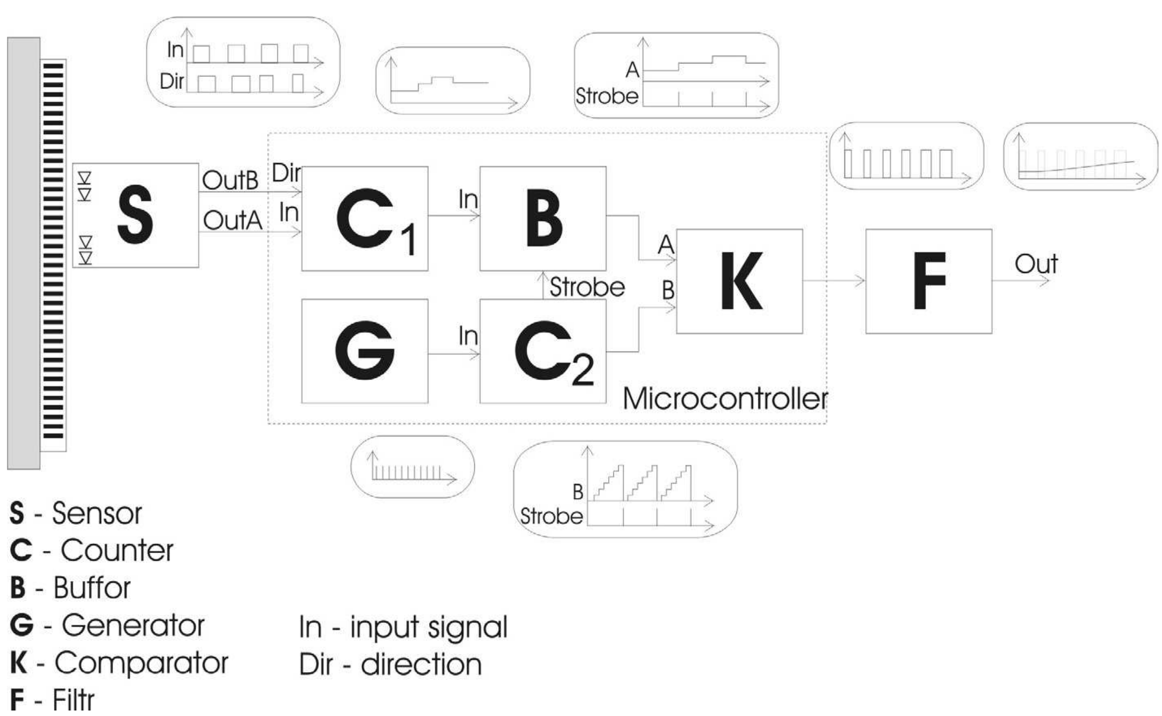

Fig. 9(b). Block diagram of displacement-voltage converter.

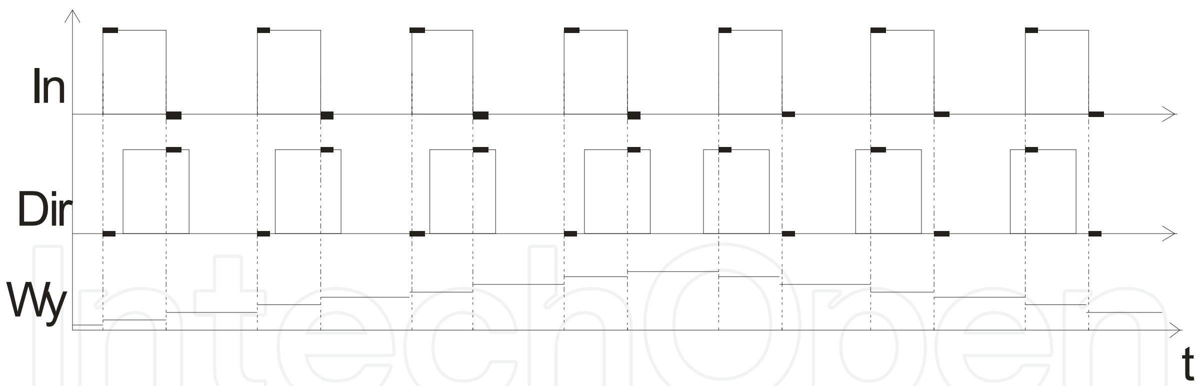

Fig. 10. The idea of pulse counting.

Sensor (S) generate series of pulses (LS) which are counted by counter (C1) and compared in comparator (K) with number of generator (G) pulses (LG) counted by counter (C2). Counter (C2) works in one direction only – the value is increased to overrun the counter. Time needed to overflow this counter determines period of generated PWM signal. PWM signal frequency is 3,5 kHz. Unless LG < LS in comparator its output is set to "high" in other case it is "low". Sensor and external microcontroller interrupt are working asynchronously. Output of pulse counter (LS) is buffered to avoid errors caused by unpredictable changes of counted value. Changing of number of pulses in buffer is possible only in moment of overflow of counter L2 (Strobe is the signal controlling this operation). This solution is hardware-implemented in timers built-in to AVR microcontrollers. The role of lowpass RC filter connected to output of PWM generator is to convert digital PWM signal into analog (average) signal. Cutoff frequency of the filter is CF=384Hz. Output buffer (operational amplifier with k=1) is conditioning signal and assure high impedance of filter load.

Control software was written in G language (LabVIEW environment). It enables to control wide variety of measurement instruments and protocols. The most popular available protocols are RS-232, USB, FireWire, LAN, GPIB, etc.). All measurement instruments, instead of IR camera which use Giga Ethernet, communicate each other by GPIB. One communication protocol enables synchronization between instruments.

Measurement scheme is divided into two loops. First loop increase heating current from minimum to maximum value with specified step; second loop decreases heating current from maximum to minimum value with the same step (See Fig.11):

$$\begin{cases} i(j) = I_{MIN} + j \cdot \Delta I \ \text{ – current increasing} \\ i(j) = I_{MIN} + (N - j) \cdot \Delta I \ \text{ – current decreasing} \end{cases} \tag{1}$$

where:
$i(j)$ – step current,
j – number of step $j \le N$,
N – number of steps,
ΔI – current step difference.

Values: N, j, ΔI are set by the user. There are ten measurement points per each step. Time between consecutive steps is set as step delay. This two direction measurement process allows for obtaining characteristics of both - direct and reverse – transitions.

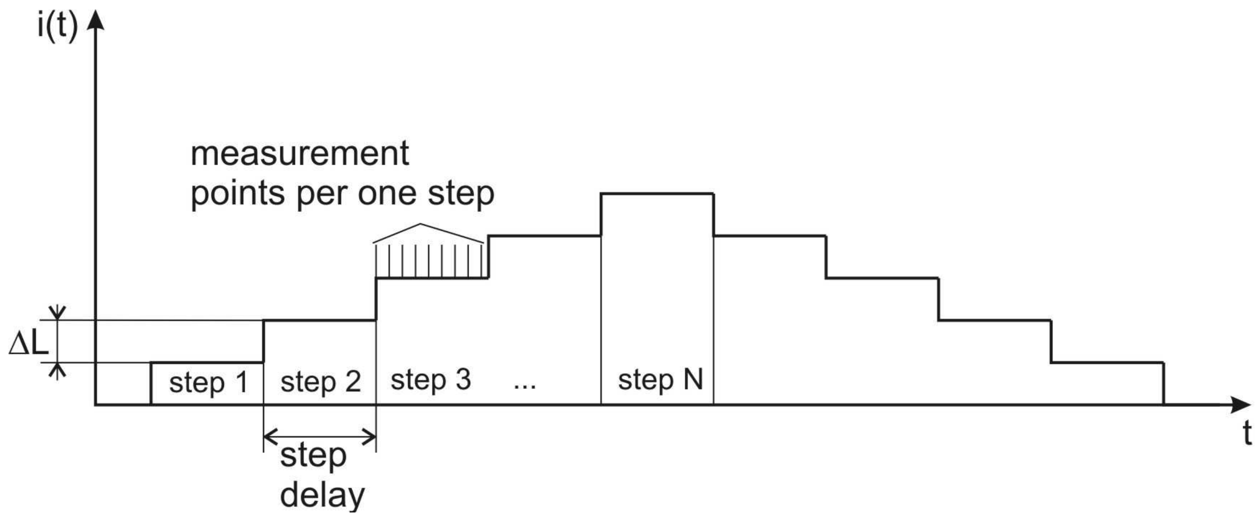

Fig. 11. The idea of measurement process.

Measurement process is triggered simultaneously using “send to group” command. Registered values of each multimeter are then acquired in serial way. Measurement algorithm of parallel triggering and serial acquisition is presented in Fig.12. Controlling algorithm is shown in Fig.13.

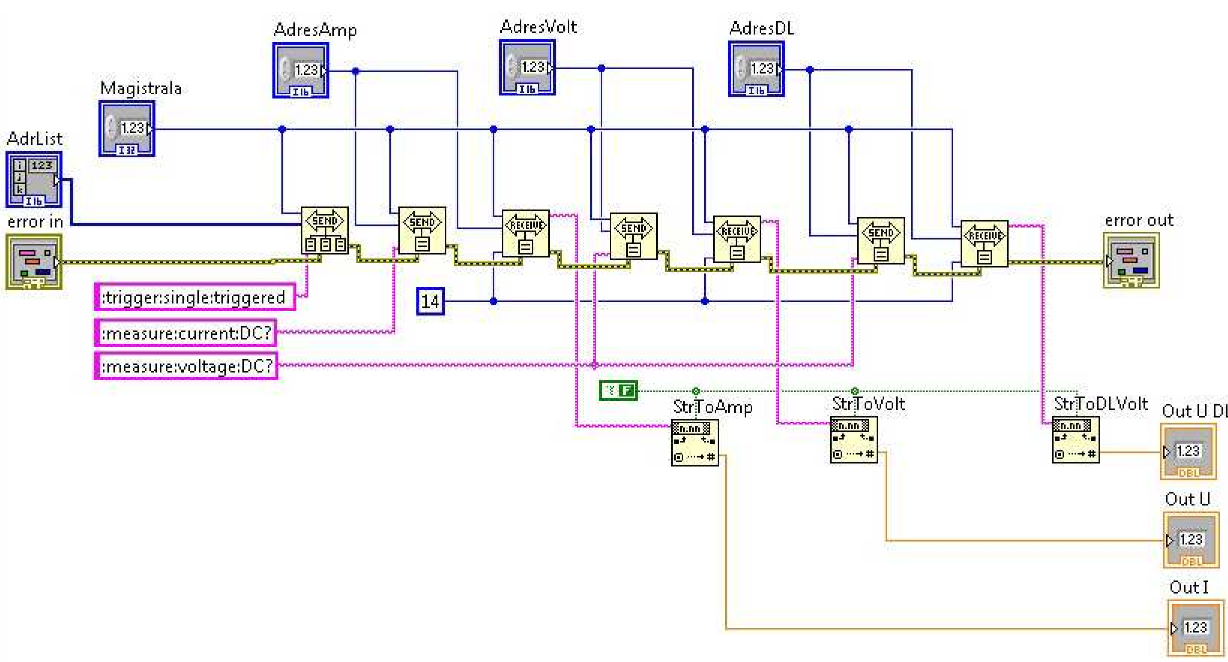

Fig. 12. Data acquisition subprogram with parallel triggering.

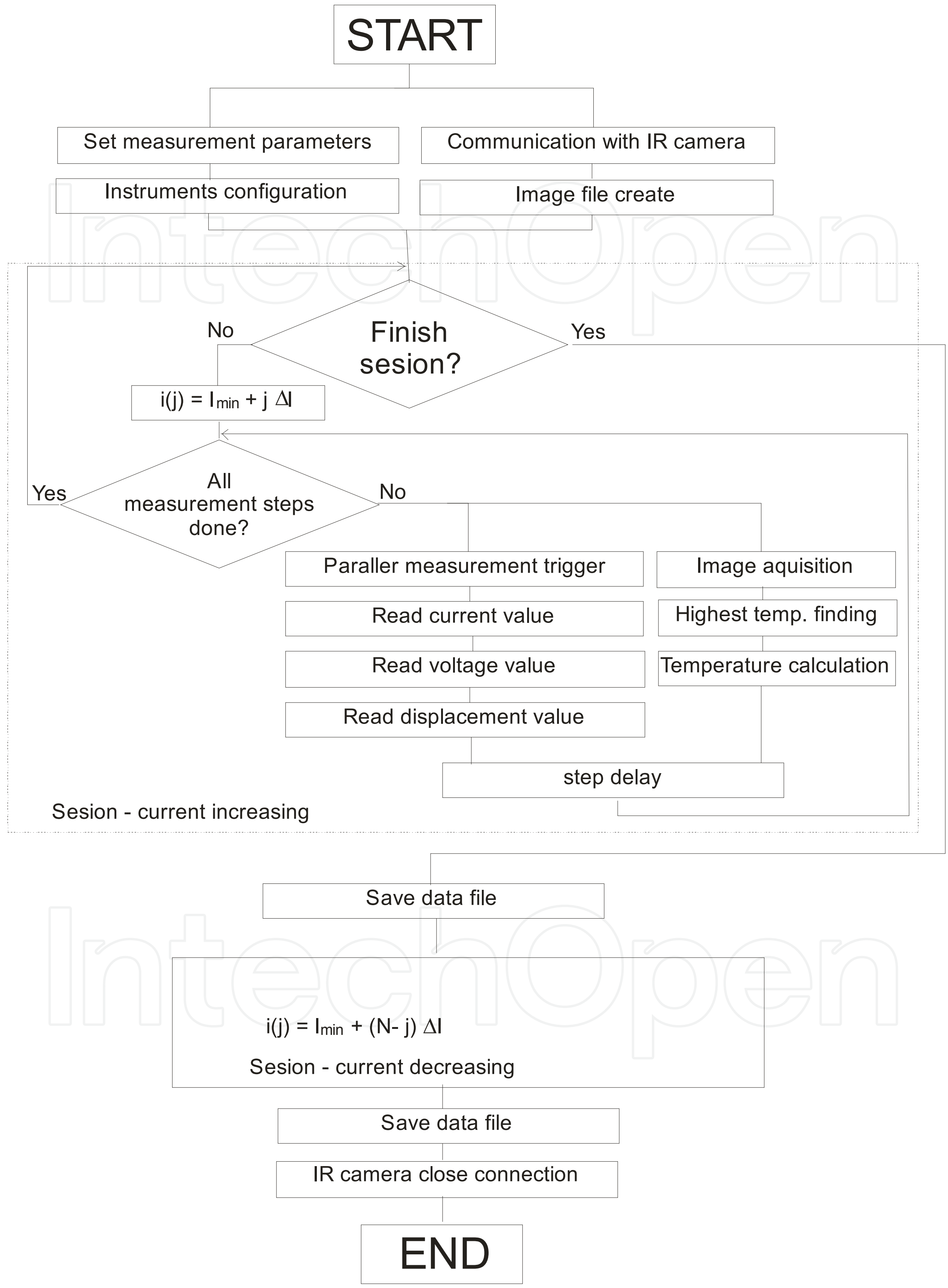

Fig. 13. Measurement algorithm.

3. Measurements accuracy

Supply current and measurements taken in the stand are executed with a specified accuracy. In the case of supply module, accuracy is related to heating current stability. Analysis of measurement accuracy of the measuring system, built with manufactured components (power supply, multimeters), is associated with the analysis of accuracy of each instrument. Accuracy of all instruments are presented in Tab. 1.

Instrument	Measurement range	Accuracy
Power supply	20A	≤ 0,2% + 10mA
	Resolution	10mA
Multimeter	200mV DCV	0,003 + 0,003
	2V DCV	0,002 + 0,0006
	20V DCV	0,002 + 0,0004
	200mA DCI	0,02 + 0,002
	1A DCI	0,02 + 0,016

Table 1. Accuracy of measuring instruments.

Heating-current stability is checked by the multimeter. Amendment for current stability is done according to following equation:

$$I = I_{set} + 5mA \pm 4mA \tag{2}$$

where:
I_{set} – current set by control unit of power supply.
Current measurement accuracy is 1mA.

Accuracy of SMA displacement consist of two parts. The first part is connected with "displacement-voltage" converter. The second one is connected with multimeter accuracy. Accuracy of "displacement-voltage" converter consist of accuracy of measurement tape – 85μm and accuracy of PWM generator. 8-bits PWM generator has 256 steps. One step is equal to 6,3mV. Accuracy of multimeter (for this measurement range) is 1mV, so it is much higher. Resulting accuracy of displacement measurement is ±1 step of measuring tape, it is equal to ±0,17mm.

4. Results and analyses

Designed measurement system allows for wide research program. All measurement results presented below concern one type of actuator. It is F2000, its nominal load is 2kg.

Some example results showing interesting characteristics and obtained relationships are shown below. All characteristics were measured at constant conditions of heat dissipation. Ambient temperature was 25±2 Celsius degrees. Cartoon shield avoided external air movement around the tested element. One static measurements cycle took approximately five hours (each step took nearby three minutes - depending on wire's diameter). Each of dynamic measurements was done in approximately ninety seconds. Measurements is finished after reaching steady state, which is defined as no change in displacement over a period of time longer than ten seconds.

4.1 Steady-state characteristics

Example result of steady-state electro-mechanical characteristic is presented in Fig.14.

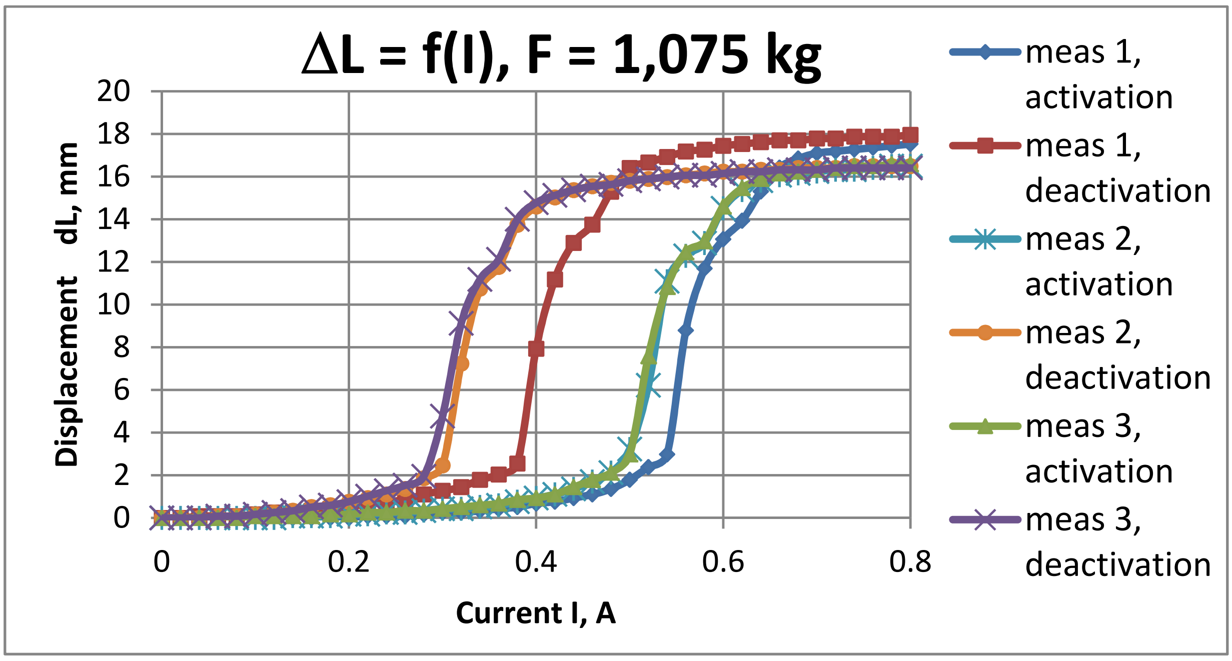

Fig. 14. Steady-state electro-mechanical characteristic.

There are three measurements called "meas 1", "meas 2", "meas 3", increasing current procedure is called "activation", decreasing current procedure is called "deactivation". Results of second and third measurement process are almost identical. Repeatability of measurement results has been analyzed. Difference between first and other results is connected with hysteresis phenomenon and history of actuator. Based on the test measurements the complete measurement procedure was determined. Full measurement procedure is presented below:

- Set the SMA actuator in the measurement stand,
- Load SMA actuator with proper mechanical bias,
- Calibration of actuator,
- Perform series of measurements.

Calibration is the process of rapid activation and deactivation of mechanically loaded actuator performed three times. It causes history cleaning before proper measurement process. Displacement measuring module is reset after calibration process. Example results obtained using developed measurement procedure are shown in Fig.15.

During measurements the question raised – what if to reverse temperature change before the transition is complete. So incomplete hysteresis loop measurements were done as well. Exemplary results are presented in Fig.16. There are results for different maximum heating currents changing in range of 0,5A to 0,8A. Full hysteresis loop is achieved for current value equal to 0,8A – it is the reference measurement. Transition starts when heating current value is about 0,4A. Each measurement was done three times. Time of martensitic transformation is independent of the rate of change of the factors causing it [6]. It means that you cannot accelerate the transition by increasing temperature (current). So process of activation performs identically each time, but halting the supply of heat energy needed to activate the actuator, stops, and even change the direction of transition.

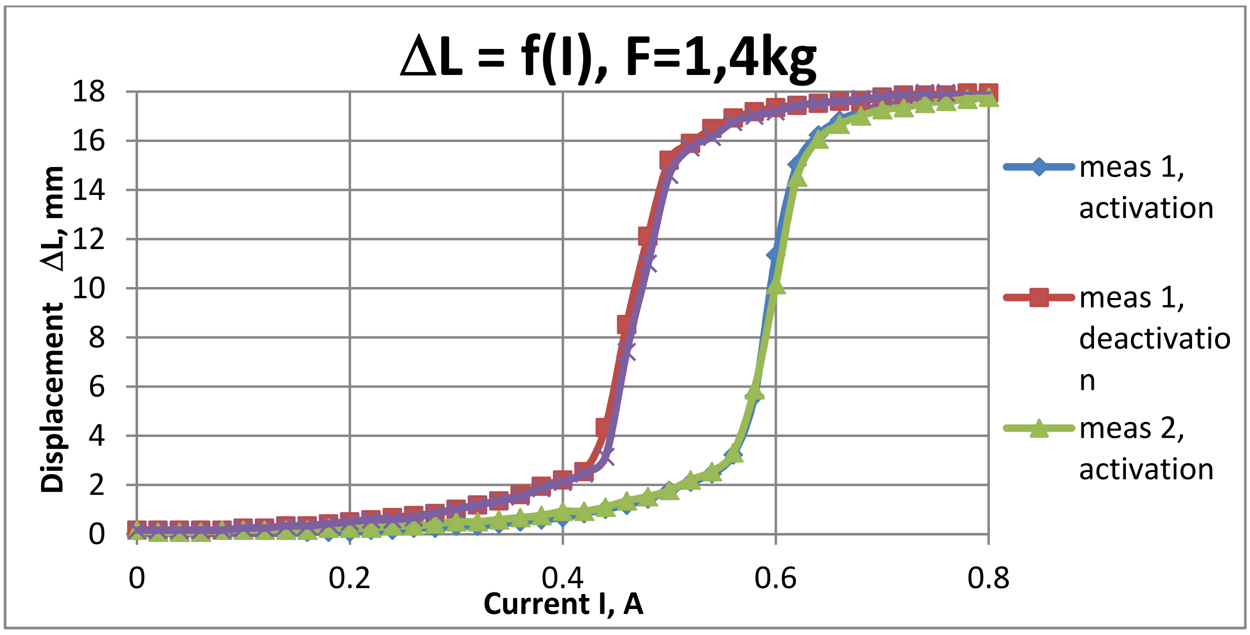

Fig. 15. Steady-state electro-mechanical characteristics acquired using developed measurement procedure (with actuator calibration).

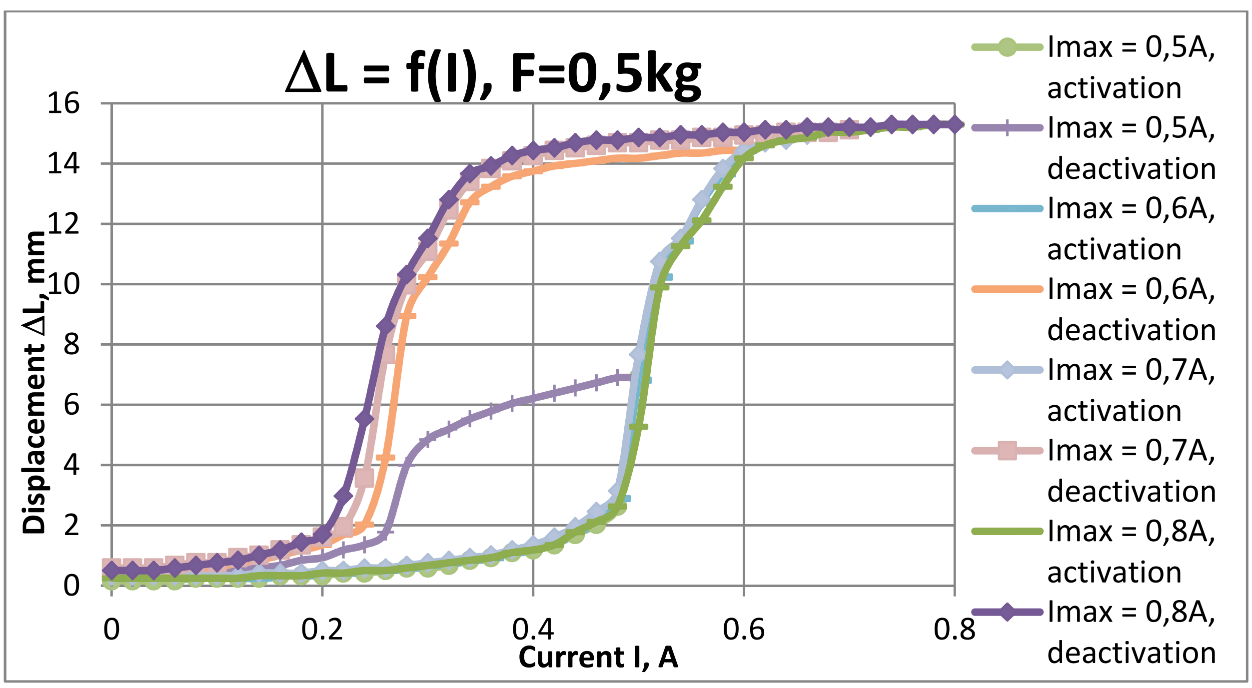

Fig. 16. Incomplete hysteresis loop measurements.

The next important characteristic of SMA actuator is load characteristic. Exemplary load characteristic is presented in Fig.17. According to the theory, increasing the mechanical load causes a linear increase of characteristic temperatures of martensitic transition while maintaining a constant width of the hysteresis loop.

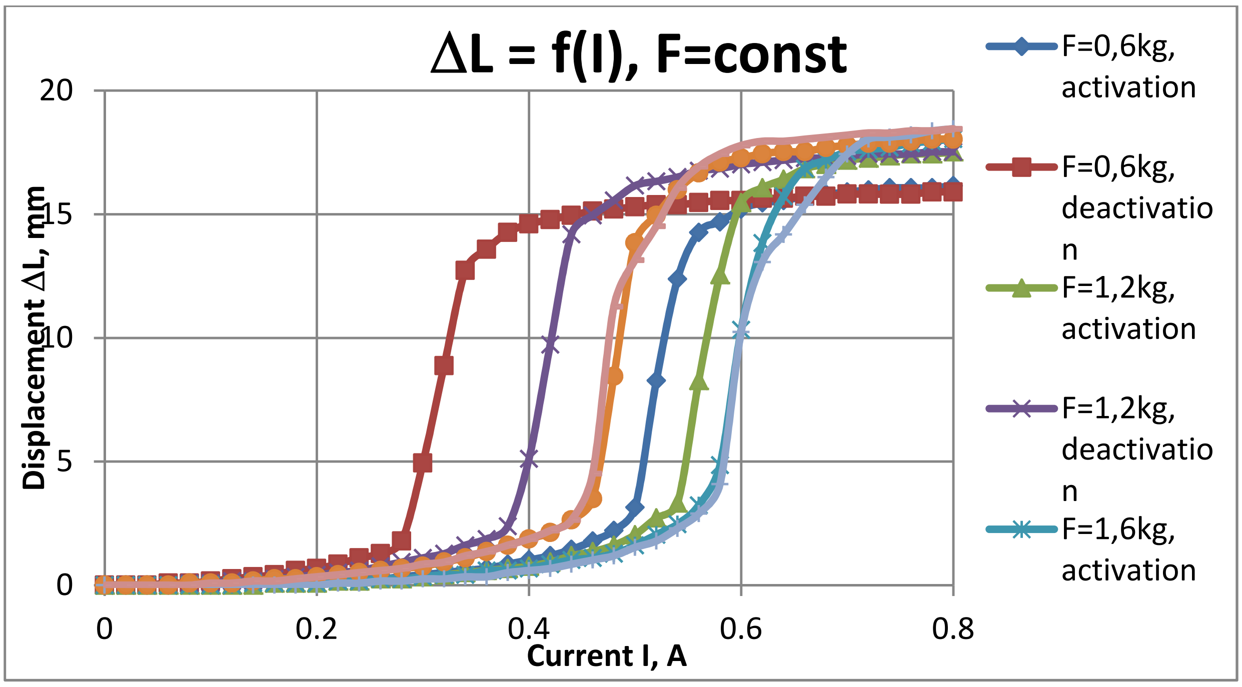

Fig. 17. Load influence on the process of martensitic transition.

It can be easily observed that higher mechanical load causes higher displacement. It is natural phenomenon connected with plastic deformation in martensitic state. Width of hysteresis loop changes according to mechanical load. For example width of hysteresis loop for 0,6kg is 0,2A (0,52A-0,32A), while it is 0,12A (0,6A-0,48A) for bias force equal to 1,6kg and 2,0 kg. It causes not linear change of important temperatures of martensitic transition.

Next interesting characteristic is electro-thermal characteristic showing relation between current and wire temperature (for constant ambient temperature). It is shown in Fig.18.

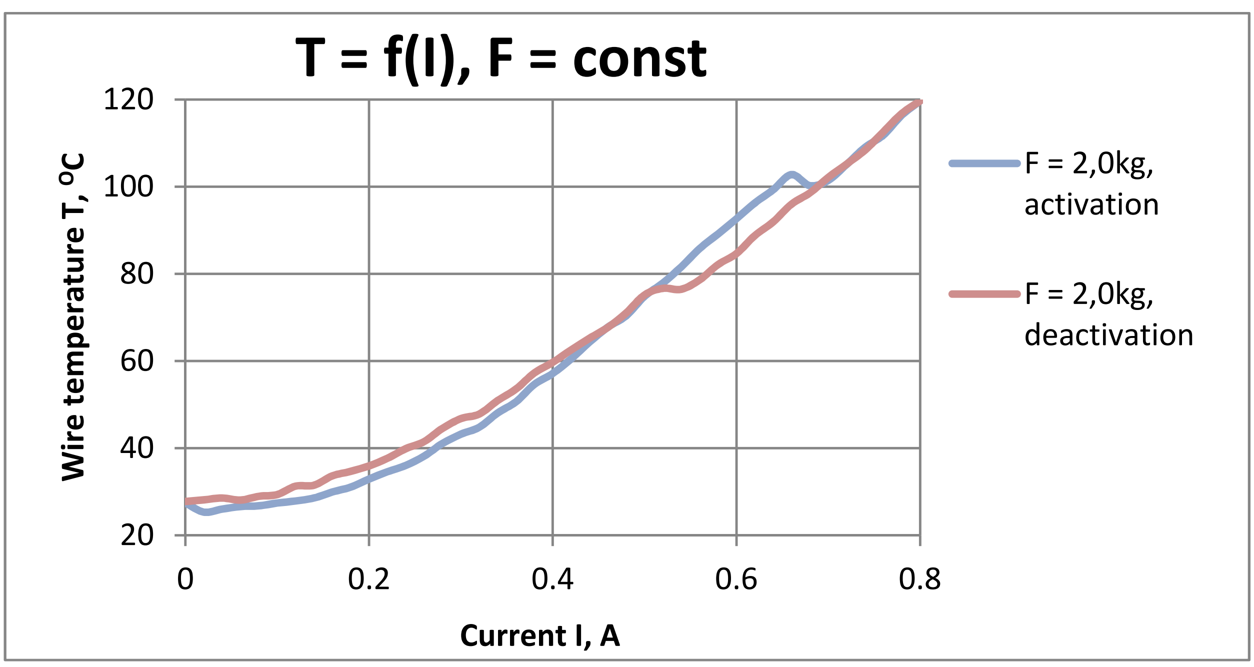

Fig. 18. Temperature vs. current characteristic, for constant ambient temperature.

Temperature characteristics of the martensitic state is a quadratic function of current. In the case of austenite, the situation is similar. A small number of measurement points in austenite state prevents the determination of the equation function. The most interesting range is the martensitic transition phase. There are different cases of temperature behavior in this state. Temperature is constant or even decreases. This is caused by consumption of thermal energy by transition process. Similar results were mentioned in [13].

Very useful characteristic is resistance as a function of heating current. In some applications the characteristics of resistance as a function of the length of the actuator are used to estimate the actual length of the actuator [12]. There are two types of resistance characteristics. First of them - resistance in function of heating current - is presented in Fig.19.

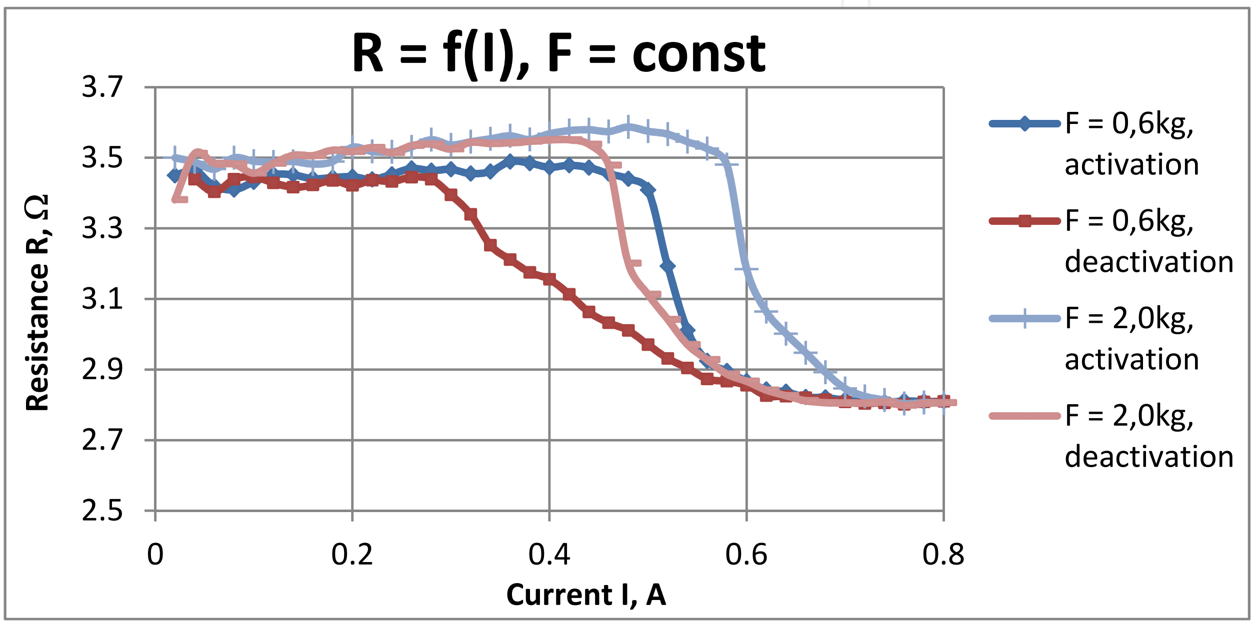

Fig. 19. Resistance vs. Current.

It is easy to notice the difference of characteristics for small and big mechanical loads (close to nominal bias force). The general rule is better noticeable for the deactivation process (direct martensitic transition). Characteristics shift toward higher currents with increasing mechanical load. This is a trend similar to the phenomenon of characteristic temperatures rising with increasing mechanical load.

Another phenomenon that can be observed is linear change of resistance with extending the wire in activation process (Fig.20). It is independent of mechanical load while for deactivation the function is linear only for mechanical load close to the nominal load. This phenomenon allows for quite accurate displacement approximation using measurements of resistance.

Simultaneous multiparameter measurement enables to plot different characteristics and a comprehensive assessment of the impact of occurring phenomena. Fig.21. shows the characteristics of displacement and temperature as a function of heating current.

The most energy consuming part of the martensitic transition is finish of activation and start of deactivation. It can happen (as can be seen in above picture) that the wire temperature decreases in spite of constant delivering of energy.

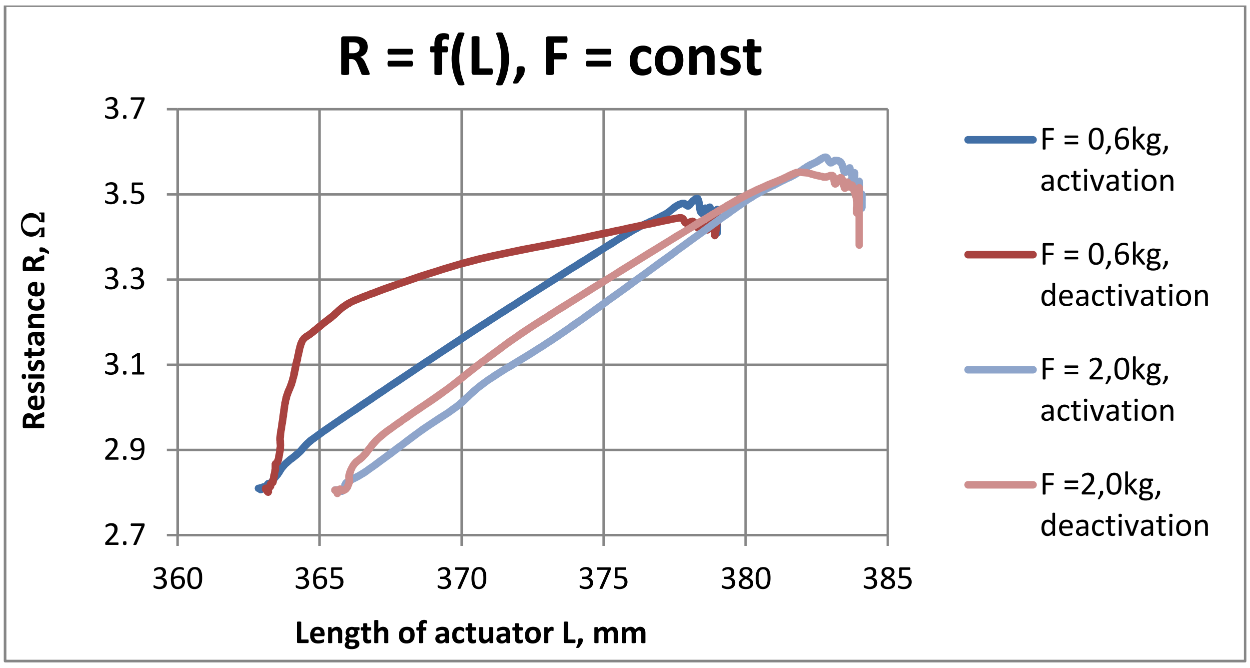

Fig. 20. Resistance vs. length of actuator.

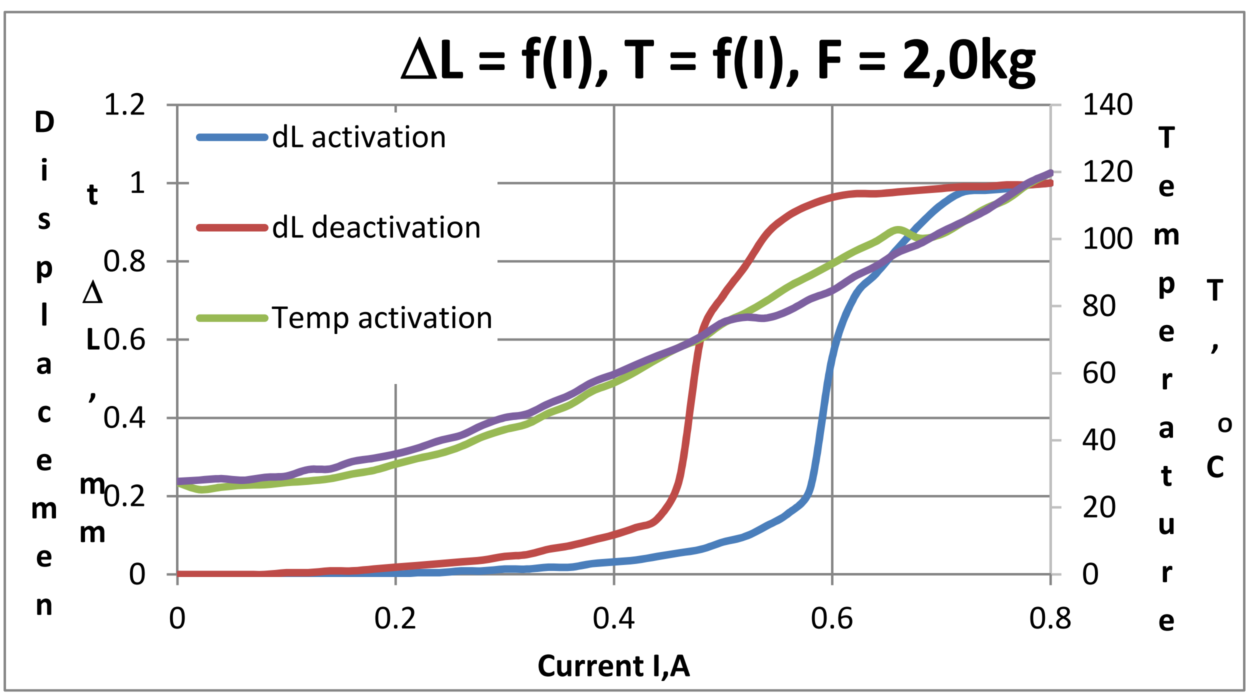

Fig. 21. Displacement and temperature characteristic vs. heating current.

4.2 Dynamic characteristics

Dynamic characteristics was acquired for two cases – switch on and switch off the heating current. In the first case dynamics of activating process is measured, in the second - dynamics of deactivating. Different mechanical bias forces and different current values have been considered. Example results are given in Fig. 22 – 25.

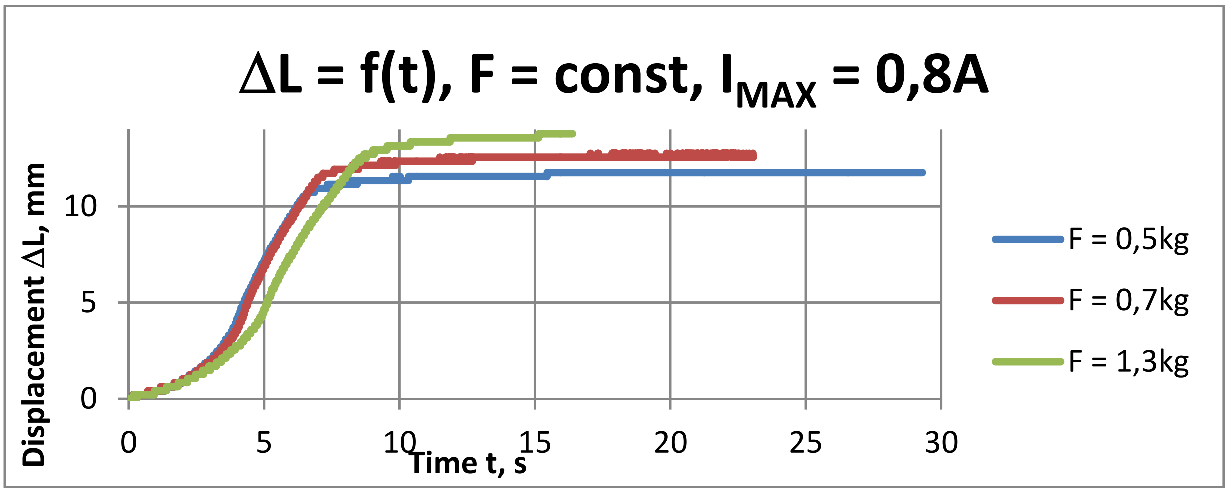

Fig. 22. Activation process for different mechanical bias forces.

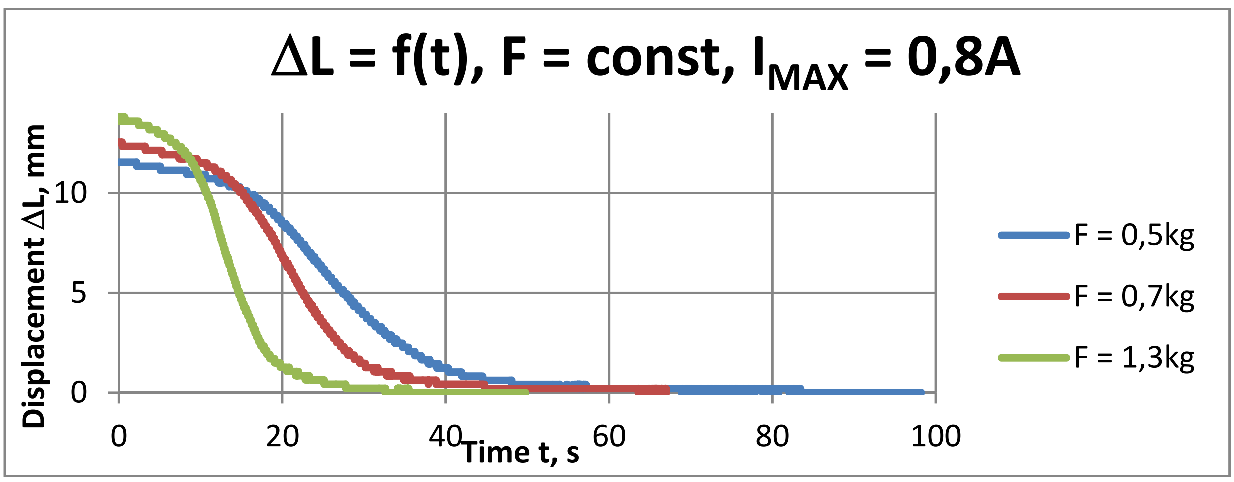

Fig. 23. Deactivation process for different mechanical bias forces.

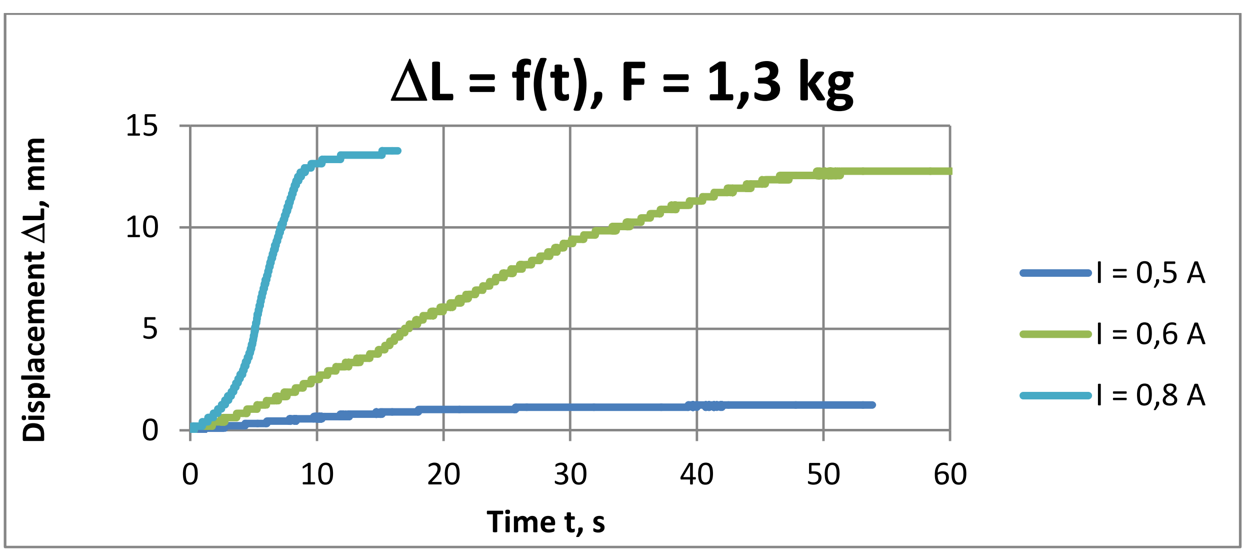

Fig. 24. Activation process for different heating currents.

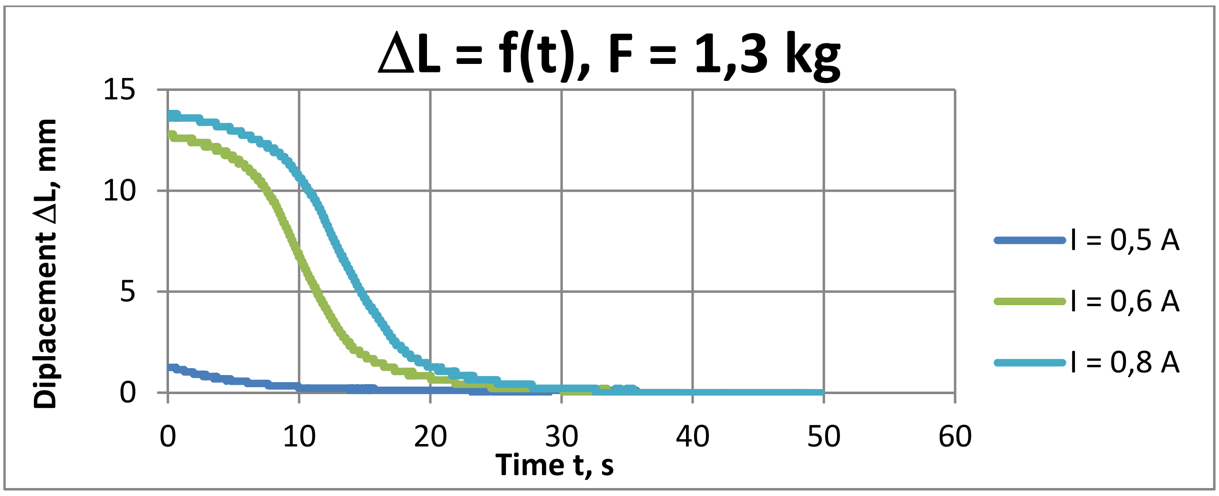

Fig. 25. Deactivation process for different heating currents.

Deactivation characteristics in Fig.23. are the result of unconstrained SMA actuator cooling. It is easy to notice the difference between time of activation and deactivation of the actuator. The higher force is, the faster actuator recovers. There is small difference in activation time, so mechanical load does not significantly affect the activation time but influence final displacement value.

Heating current value significantly influences the speed of the activation process. Current value 0,8A causes full activation, lower values does not. There is not big difference in final displacement between heating current values 0,6A and 0,8A, but time is important factor. The slope of the deactivation curve does not depend on the starting point but is strongly connected with conditions of heat dissipation.

5. Conclusions

Designed measurement stand can be very helpful in research of Shape Memory Effect. It allows for simultaneous multiparameter measurement which enables to draw various characteristics of SMA wire actuators. Presented characteristics prove the utility of designed measurement systems. It is possible to compare different characteristics of the SMA actuator for one forced parameter (e.g. comparison of the displacement and wire temperature as a function of heating current (Fig.21)). Using some dependences that occur among certain physical quantities it is also possible to calculate some additional parameters and draw additional characteristics (e.g. resistance as function of current or actuator length (Fig.18 and Fig.19)).

Design of the stand allows for performance of reach research program. Measurement process is performed in semiautomatic way. User has to set measurement parameters described in (1) and start the process. All current changes and data acquisition is done automatically which increase measurement accuracy. Automatic operation save a lot of time and eliminates the distortions arising from the presence of people close to measurement system (e.g. air movement around heated wire). Moreover process parameters can be changed remotely (using Internet) which means that it is possible to obtain whole family of characteristics without physical access to the stand. The use of virtual measuring instruments and computer control makes it easy to develop the measuring stand. Some planned developments of the measuring stand would give:

- the ability to automatically adjust mechanical load,
- the opportunity to ask about specific mechanical load parameters (time or displacement),
- possibility to adjust air movement,
- automatic measurement of environmental conditions (temperature, pressure, humidity),
- possibility of automatic adjusting environmental conditions.

The stand was co-financed with governmental founds (project number N N510 353036).

6. References

[1] Kciuk M.: *Computer based measurement system for shape memory alloy*. IX International Workshop for Candidates for Doctor's Degree OWD'2007, Wisła 20-23.10.2007, str. 177-180,

[2] Koji Ikuta, Masahiro Tsukumoto, Shigeo Hirose: *Shape memory alloy servo actuator system with electric resistance feedback and application for active endoscope*. CH2555-1/88/0000/0427$01.00 0 1988 IEEE

[3] Krzysztof Biereg: *Porównanie wybranych równań konstytutywnych stopów z pamięcią kształtu*. Modelowanie inżynierskie, Gliwice 2006.

[4] Koji Ikuta, Masahiro Tsukamoto, Shigeo Hirose: *Mathematical model and experimental verification of Shape Memory Alloy for designing micro actuator*. IEEE 1991

[5] Koji Ikuta, Hidenori Shimizu: *Two dimensional mathematical model of Shape Memory Alloy and intelligent SMA-CAD*. IEEE 1993.

[6] Ziółkowski A.: *Pseudoelastyczność stopów z pamięcią kształtu badania doświadczalne i opis teoretyczny*. Praca habilitacyjna, IPPT PAN, Warszawa 2006.

[7] Kyu-Jin Cho, Harry H. Assada: *Multi-axis SMA actuator array for driving anthropomorphic robot hand*. International Conference on Robotics & Automation, Spain, April, 2005.

[8] Liu C.Y., Liao W. H.: *A snake robot using Shape Memory Alloys*. International Conference on Robotics and Biomimetics Shenyang, China, August 22-26, 2004, Proceedings of the 2004 IEEE.

[9] Masaru Fujii, Hiroshi Yokoi: *Modeling and movement control of mobile SMA-Net*. International Symposium on Computational Inteligence in Robotics and Automation, Kobe, Japan, July, 16-20, 2003, Proceedings 2003 IEEE.

[10] Ikuta K.: *Micro/miniature Shape Memory Alloy actuator*. CH2876-1/90/0000/2156$01.00 0 1990 IEEE.

[11] Technical data for sensor H9720 *http://www.avagotech.com/docs/AV02-0511EN*

[12] Zurbitu J., Kustov S., Zabaleta A., Cesari E., Aurrekoetxea J.: *Thermo-mechanical behavior of NiTi at impact. Shape Memory Alloys*. ISBN 978-953-307-106-0, publishing date: October 2010

[13] Kciuk M., Kłapyta G.: *Koncepcja stanowiska pomiarowego do wyznaczania charakterystyk elektro-termo-mechanicznych stopów z pamięcią kształtu (SMA)*. Materiały XIII Sympozjum „Podstawowe Problemy Energoelektroniki, Elektromechaniki i Mechatroniki" PPEEm 2009, Wisła 14-17.12.2009, str. 242-247.

[14] Hui Li, Chen-Xi Mao Jin-Ping Ou: *Experimental and theoretical study on two types of Shape Memory Alloy devices*. Earthquake Engineering And Structural Dynamics 19 September 2007 in Wiley InterScience (www.intersciecnce.wiley.com).

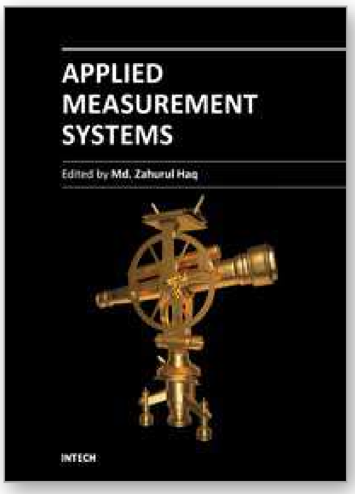

Applied Measurement Systems
Edited by Prof. Zahurul Haq

ISBN 978-953-51-0103-1
Hard cover, 390 pages
Publisher InTech
Published online 24, February, 2012
Published in print edition February, 2012

Measurement is a multidisciplinary experimental science. Measurement systems synergistically blend science, engineering and statistical methods to provide fundamental data for research, design and development, control of processes and operations, and facilitate safe and economic performance of systems. In recent years, measuring techniques have expanded rapidly and gained maturity, through extensive research activities and hardware advancements. With individual chapters authored by eminent professionals in their respective topics, Applied Measurement Systems attempts to provide a comprehensive presentation and in-depth guidance on some of the key applied and advanced topics in measurements for scientists, engineers and educators.

InTech Europe
University Campus STeP Ri
Slavka Krautzeka 83/A
51000 Rijeka, Croatia
Phone: +385 (51) 770 447
Fax: +385 (51) 686 166
www.intechopen.com

InTech China
Unit 405, Office Block, Hotel Equatorial Shanghai
No.65, Yan An Road (West), Shanghai, 200040, China
中国上海市延安西路65号上海国际贵都大饭店办公楼405单元
Phone: +86-21-62489820
Fax: +86-21-62489821